J|A|C|S
ARTICLES
Published on Web 03/08/2003

# Oxygen Equilibrium Properties of Myoglobin Locked in the Liganded and Unliganded Conformations

Naoya Shibayama* and Satoshi Saigo

*Contribution from the Department of Physiology, Division of Biophysics, Jichi Medical School, Yakushiji 3311-1, Minamikawachi, Kawachi, Tochigi 329-0498, Japan.*

Received November 6, 2002; E-mail: shibayam@jichi.ac.jp

***Abstract:*** A comparison of the $O_2$ equilibrium curves of sperm-whale myoglobin locked in the liganded (CO-bound) and unliganded (deoxy) conformations by encapsulation in a wet porous sol−gel silica reveals a marked difference between them. The CO-bound state-locked myoglobin showed a nearly monophasic (hyperbolic) $O_2$ equilibrium curve with a dissociation constant of 0.2 Torr, which is smaller than that of myoglobin in solution (0.5 Torr). On the other hand, the deoxy state-locked myoglobin exhibited a multiphasic $O_2$ equilibrium curve that can be represented by a sum of three independent components with dissociation constants of 0.19, 0.90, and 44 Torr, respectively, indicating that deoxymyoglobin exists in multiple conformations. These results show that myoglobin can be frozen into ligand-dependent conformational populations at room temperature in the wet sol−gel and suggest that the overall $O_2$ equilibrium properties of myoglobin in solution are generated by a redistribution of protein conformational populations in response to ligand binding.

## Introduction

Myoglobin (Mb), a small $O_2$ storage heme protein that binds $O_2$ (or CO) reversibly at the ferrous heme iron, is an important model system for studying the molecular mechanism of ligand binding reactions in proteins. Of particular interest is the role of the protein structures in controlling the affinity for ligands. Recent studies show that Mb can adopt different tertiary conformations. For example, a comparison of the X-ray crystallographic structures of unliganded Mb (deoxyMb) and CO-liganded Mb (MbCO) at near-atomic resolution shows that there are small motions of the E and F helices in going from the unliganded to liganded conformation.[1] Ultraviolet resonance Raman studies also indicate that the N- and C-terminal regions in Mb undergo structural changes upon CO binding.[2] Moreover, recent time-resolved Laue X-ray diffraction studies demonstrate that very fast protein relaxation involving the E and F helices is evident at 1 ns after photolysis of the crystal of MbCO at room temperature.[3] In addition to the above global structural differences, there are additional structural differences in the local heme environment between the equilibrium deoxyMb and the nonequilibrium deoxyMb derivative derived from the photolysis of MbCO, as probed by a variety of spectroscopic techniques, including optical absorption,[4] magnetic susceptibility,[5] infrared,[6] resonance Raman,[7] and circular dichroism measurements.[8] Though informative, these structural data have not directly led to a clear understanding of how these different tertiary conformations impact ligand binding. In this paper we address this issue by investigating the $O_2$ equilibrium properties of Mb locked in the liganded and unliganded conformations.

We use a recently developed method of trapping the conformations of proteins by encapsulation in a transparent wet porous sol−gel silica.[9−18] This gel matrix provides a means of slowing large-scale protein motions,[11−13] while the encapsulated protein molecules are solvated and retain their properties in solution.[9−18] As a result, the protein conformations *in solution* can be effectively trapped. It has been already established that the wet sol−gel is capable of maintaining the quaternary structures of fully liganded,[9,17] half-liganded,[11] and fully unliganded hemoglobin molecules[9,10,16] during the $O_2$ equilibrium measurements. The applicability of the sol−gel method for trapping the tertiary conformations of Mb was recently inves-

(1) Kachalova, G. S.; Popov, A. N.; Bartunik, H. D. *Science* **1999**, *284*, 473−476.
(2) Haruta, N.; Aki, M.; Ozaki, S.; Watanabe, Y.; Kitagawa, T. *Biochemistry* **2001**, *40*, 6956−6963.
(3) Srajer, V.; Ren, Z.; Teng, T.-Y.; Schmidt, M.; Ursby, T.; Bourgeois, D.; Pradervand, C.; Schildkamp, W.; Wulff, M.; Moffat, K. *Biochemistry* **2001**, *40*, 13802−13815.
(4) (a) Iizuka, T.; Yamamoto, H.; Kotani, M.; Yonetani, T. *Biochim. Biophys. Acta* **1974**, *371*, 126−139. (b) Ansari, A.; Jones, C. M.; Henry, E. R.; Hofrichter, J.; Eaton, W. A. *Biochemistry* **1994**, *33*, 5128−5145.
(5) Roder, H.; Berendzen, J.; Bowne, S. F.; Frauenfelder, H.; Sauke, T. B.; Shyamsunder, E.; Weissman, M. B. *Proc. Natl. Acad. Sci. U.S.A.* **1984**, *81*, 2359−2363.
(6) Fiamingo, F. G.; Alben, J. O. *Biochemistry* **1985**, *24*, 7964−7970.
(7) Rousseau, D. L.; Argade, P. V. *Proc. Natl. Acad. Sci. U.S.A.* **1986**, *83*, 1310−1314.
(8) Xie, X. L.; Simon, J. D. *Biochemistry* **1991**, *30*, 3682−3692.
(9) Shibayama, N.; Saigo, S. *J. Mol. Biol.* **1995**, *251*, 203−209.
(10) Bettati, S.; Mozzarelli, A. *J. Biol. Chem.* **1997**, *272*, 32050−32055.
(11) Shibayama, N. *J. Mol. Biol.* **1999**, *285*, 1383−1388.
(12) Shibayama, N.; Saigo, S. *J. Am. Chem. Soc.* **1999**, *121*, 444−445.
(13) Das, T. K.; Khan, I.; Rousseau, D. L.; Friedman, J. M. *Biospectroscopy* **1999**, *5*, S64−S70.
(14) Juszczak, L. J.; Friedman, J. M. *J. Biol. Chem.* **1999**, *274*, 30357−30360.
(15) Khan, I.; Shannon, C. F.; Dantsker, D.; Friedman, A. J.; Perez-Gonzalez-de-Apodaca, J.; Friedman, J. M. *Biochemistry* **2000**, *39*, 16099−16109.
(16) Shibayama, N.; Saigo, S. *FEBS Lett.* **2001**, *492*, 50−53.
(17) Shibayama, N.; Miura, S.; Tame, J. R. H.; Yonetani, T.; Park, S.-Y. *J. Biol. Chem.* **2002**, *277*, 38791−38796.
(18) Samuni, U.; Dantsker, D.; Khan, I.; Friedman, A. J.; Peterson, E.; Friedman, J. M. *J. Biol. Chem.* **2002**, *277*, 25783−25790.


**10.1021/ja029237g CCC: $25.00** 

tigated by Samuni et al.,[18] who found that the 8-ns photoproducts from two horse MbCO samples that were initially encapsulated in the CO-liganded and deoxy form, respectively, differ in their iron-proximal His(F8−93) stretching frequency and CO rebinding kinetics. In this study, we demonstrate that the $O_2$ equilibrium properties of sperm-whale Mb derivatives locked in the liganded (CO-bound) and unliganded (deoxy) conformations within the wet sol−gel are markedly different from each other. The structural origins of the $O_2$ binding characteristics of the individual protein conformations and their possible contribution to the protein function are discussed.

## Experimental Procedures

The major component of sperm-whale Mb was isolated by DEAE cellulose column chromatography according to the method of Yamazaki et al.[19] The silica sol was synthesized from tetramethyl orthosilicate (Tokyo Kasei Company) as previously described.[9] The sol was mixed with 1.5 volumes of 1.1% (w/v) sperm-whale ferric cyanomet Mb in 50 mM potassium phosphate buffer, pH 7.0, with 10 mM KCN, in a rotating sealed glass tube (1 cm diameter). Gelation occurred within 4 min at 0 °C. The resultant cyanomet Mb-doped thin film (i.e., 0.02−0.05 mm thickness), which adhered to the inner surface of the glass tube, was soaked in 0.1 M potassium phosphate buffer, pH 7.0 (without KCN), and was allowed to stand at 0 °C for 1 h. Two such samples were prepared. One was then converted to the deoxy form by immersion in Ar-saturated 0.1 M potassium phosphate buffer, pH 7.0, in the presence of 2 mM sodium dithionite, followed by equilibration at 35 °C for 45 h. The other was converted to the CO-bound form by immersion in CO-saturated 0.1 M potassium phosphate buffer, pH 7.0, in the presence of 2 mM sodium dithionite, followed by equilibration at 35 °C for 45 h. The equilibrated deoxy (or CO-bound) sample was washed with dithionite-free buffer and was immersed in a buffered silica sol composed of 1 volume of Ar-saturated (or CO-saturated) tetramethyl orthosilicate and 7.5 volumes of Ar-saturated (or CO-saturated) 0.1 M potassium phosphate buffer, pH 7.0, containing 2 mM dithionite. After 6 min of incubation at 0 °C, the excess silica sol was discarded. Then the sample was left at 0 °C for 20 min. At this stage, the second sol−gel had formed in the pores of the original sol−gel films. The resultant sol−gel sample was washed with Ar-saturated (or CO-saturated) 0.1 M potassium phosphate buffer, pH 7.0, in the presence of 2 mM sodium dithionite, followed by equilibration at 35 °C for 45 h. Note that, in the case of the CO-bound state-locked Mb, the bound CO was removed by the method described previously[12] immediately before the $O_2$ equilibrium measurement.

The $O_2$ equilibrium measurements were carried out by exposing the Mb-doped sol−gel thin films to defined $O_2$ pressures at 20 °C. The equilibrium with $O_2$ was usually completed within 3−60 min (the necessary time for equilibration depends on the concentration of $O_2$). The increment of the met Mb content during the measurements was always less than 10%. Other experimental details are essentially the same as those described previously.[16]

## Results

In the present study, sol−gel trapping of sperm-whale Mb in the CO-liganded and deoxy conformations was carried out by a modified method of Shibayama[11] for encapsulation of hemoglobin. The absorption spectra of the resulting Mb samples in the sol−gel were very similar to those of the corresponding solution-phase samples, indicating that the protein conformation is not significantly altered by the sol−gel matrix.

An underlying requisite for determination of the $O_2$ equilibrium properties of a "trapped" protein conformation is that the ligation-linked conformational change is slower than the time scale of the $O_2$ equilibrium measurement. We therefore investigated the kinetics of the conformational relaxation of Mb in our sol−gel. The relaxation was initiated by rapid deoxygenation of an $O_2$-liganded Mb ($MbO_2$) sample with sodium dithionite[12] to produce a nonequilibrium deoxyMb having a conformation of the liganded state. Figure 1 shows the time-dependent Soret spectral change of such a deoxyMb sample in going from the liganded to the unliganded conformation in the sol−gel. This spectral change can be explained as reflecting the shift of the Soret band peak from 435.4 to 434.0 nm on the hour to day time scale and is similar in shape to that observed for the difference between the submillisecond $O_2$ photoproduct of sperm-whale Mb (generated by a 6-ns laser pulse) and the equilibrium deoxyMb in solution.[20] We also found that this Soret band shift is nonexponential in time, in agreement with the previous observation of the spectral relaxation of deoxyMb following photolysis of sperm-whale MbCO in viscous solvents at 250−290 K.[21] Thus, we interpret these observations as evidence that the sol−gel matrix considerably slows down the conformational relaxation of Mb.

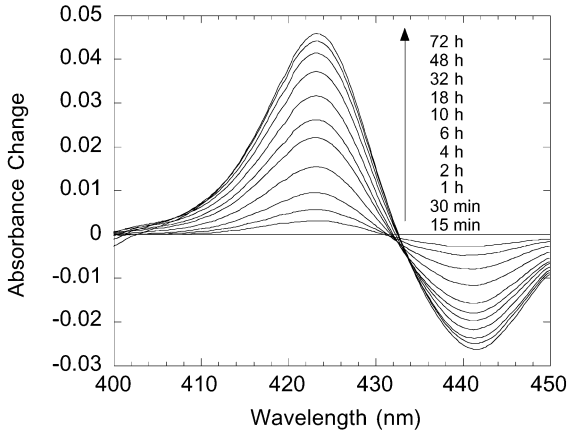


***Figure 1.*** Transient difference spectra of the sol−gel encapsulated sperm-whale deoxyMb in going from the liganded to the unliganded conformation in the presence of 0.1 M potassium phosphate buffer, pH 7.0, at 20 °C. The spectrum measured after 5 min of the deoxygenation period was used as reference (defined as $t = 0$) in order to eliminate the initial lag due to the diffusion of dithionite into the gel. The difference spectra measured at 15 min, 30 min, and 1, 2, 4, 6, 10, 18, 32, 48, and 72 h are shown.

On the basis of these observations, we determined the $O_2$ equilibrium curves of Mb locked in the CO-liganded and deoxy conformations in the sol−gel before the ligation-linked structural change takes place to any significant degree (see Experimental Procedures). Figure 2 shows the Hill plots of these results. Reversibility of each equilibrium curve was confirmed by agreement between the oxygenation data (solid symbols) and the corresponding deoxygenation data (open symbols). The excellent agreement of the association and dissociation data implies that we actually observed an "$O_2$ equilibrium".

Remarkably, the $O_2$ equilibrium properties of Mb locked in the liganded and unliganded conformations are different from each other (Figure 2). The CO-bound state-locked Mb exhibits a very high affinity for $O_2$ (i.e., $P_{50} = 0.2$ Torr; $P_{50}$ is $O_2$ pressure at half saturation), which is even higher than that of Mb in solution[22] ($P_{50} = 0.5$ Torr; see the straight broken line

(19) Yamazaki, I.; Yokota, K.; Shikama, K. *J. Biol. Chem.* **1964**, *239*, 4151−4153.

(20) Sato, F.; Shiro, Y.; Sakaguchi, Y.; Suzuki, T.; Iizuka, T.; Hayashi, H. *J. Biol. Chem.* **1990**, *265*, 2004−2010.

(21) Franzen, S.; Boxer, S. G. *J. Biol. Chem.* **1997**, *272*, 9655−9660.

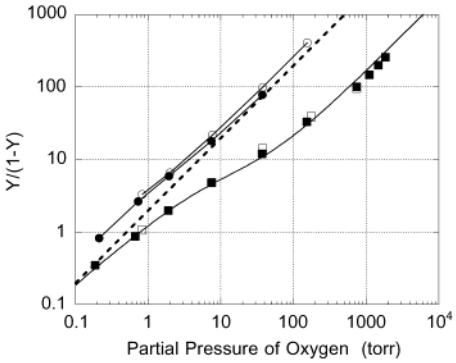


***Figure 2.*** Hill plots for $O_2$ equilibrium curves of sol−gel encapsulated sperm-whale Mb locked in the CO-bound state (circles) and deoxy state (squares) in the sol−gel containing 0.1 M potassium phosphate buffer, pH 7.0, at 20 °C. The fractional saturation with $O_2$ ($Y$) was calculated from the absorbance values at 430 nm. Solid symbols represent the $O_2$ association curves; open symbols represent the $O_2$ dissociation curves. The straight broken line is the Hill plot of the $O_2$ equilibrium curve for sperm-whale Mb in solution at pH 7.0, at 20 °C.[22] The solid line joining the squares is the result of analysis assuming the presence of three independent components with different $O_2$ dissociation equilibrium constants. The $O_2$ dissociation equilibrium constants of 0.19 Torr (27%), 0.90 Torr (60%), and 44 Torr (13%) were obtained (the fractional populations are shown in the parentheses).

in Figure 2). As shown in Figure 2, the $O_2$ equilibrium curve of the CO-bound state-locked Mb shows a Hill coefficient close to unity, indicating that the trapped Mb molecules exhibit a similar $O_2$ affinity. By contrast, the $O_2$ equilibrium curve of the deoxy state-locked Mb exhibits a relatively low affinity ($P_{50}$ = 0.8 Torr) and a Hill coefficient less than unity (see Figure 2), indicating that deoxyMb exists in multiple conformations with different $O_2$ affinities. Our analysis indicates that at least three independent components with different $O_2$ affinities are required to fit the $O_2$ equilibrium curve of the deoxy state-locked Mb. The obtained $O_2$ dissociation constants for these three components are 0.19, 0.90, and 44 Torr, respectively.

To eliminate the possibility that the observed functional heterogeneity in the deoxy state-locked Mb is an artifact of microscopic heterogeneity of the sol−gel interior, the deoxy state-locked Mb was converted to the CO form and warmed to 35 °C to facilitate conformational mobility[11,13] and then allowed to stand at 35 °C for 40 h (reequilibration). After the reequilibration, the $O_2$ association curve became very similar to that for the CO-bound state-locked Mb (data not shown), indicating that microscopic heterogeneity of the sol−gel, if any, is not an essential determinant of the affinity states of Mb. We also confirmed that the $O_2$ equilibrium characteristics of the CO-bound state-locked Mb in the sol−gel could be converted to those of the deoxy state-locked Mb by 40 h of deoxy reequilibration at 35 °C (data not shown).

## Discussion

**Effects of Sol−Gel Encapsulation.** Our results demonstrate that Mb can be frozen into ligand-dependent conformational populations at room temperature in the wet sol−gel (Figures 1 and 2). We have shown that the $O_2$ equilibrium properties of Mb locked in the liganded (CO-bound) and unliganded (deoxy) conformations by encapsulation in the wet sol−gel are markedly different from each other (Figure 2). Since this sol−gel matrix provides a means of inhibiting large-scale protein motions, the observed functional differences between these two states are likely due to global structural differences. Recent near-atomic resolution X-ray studies on MbCO and deoxyMb show that CO binding requires global motions of the E and F helices in relation to the heme.[1] Perhaps our sol−gel inhibits these motions, which may be coupled to changes in both the proximal and distal environments of the heme. In fact, recent resonance Raman studies on the 8-ns photoproducts of sol−gel encapsulated horse MbCO derivatives show that the iron-proximal His(F8−93) stretching frequency is 1−2 $cm^{-1}$ lower (more strained) in the deoxy conformation than in the CO-liganded conformation,[18] suggesting a difference in the positioning of the F-helix between these two conformations.

**Heterogeneity in DeoxyMb.** The key question remains: why does the deoxy state-locked Mb show multiple conformations with different $O_2$ affinities? The $O_2$ affinities of the deoxyMb conformations range widely from about 0.2 to 40 Torr (Figure 2). Nevertheless, there is no evidence of heterogeneity in the iron-proximal His(F8−93) stretching Raman line for the deoxyMb samples in sol−gels and in solution.[18] On the other hand, there is an obvious correlation between the functional heterogeneity in the sol−gel encapsulated Mb samples and the multiplicity of the distal heme pocket conformations that are observed in the crystal structures at room temperature.[1] In deoxyMb the distal His(E7−64) side chain adopts at least two conformations that significantly differ in their distance from the ligand binding site of the heme iron, whereas in MbCO it adopts a single conformation at room temperature.[1] Since the distal heme pocket conformation directly influences $O_2$ affinity by steric hindrance and by hydrogen bonding between bound $O_2$ and the distal His(E7−64),[23−25] the distal heme pocket conformational populations would lead to significant functional heterogeneity.

Additional evidence supporting this correlation comes from our recent findings on a sol−gel encapsulated Mb sample locked in the ferric, water-liganded conformation (aquomet state-locked Mb). In aquomet Mb, the distal His(E7−64) side chain adopts only a single conformation which is stabilized by hydrogen bonding to the ligand water,[26] whereas the position of the iron relative to the heme plane is intermediate between that of MbCO and deoxyMb because the iron is in high-spin state.[26] Our data show that the aquomet state-locked Mb exhibits a simple monophasic (hyperbolic) $O_2$ equilibrium curve with a dissociation constant of 0.9 Torr (data not shown), which is significantly larger (lower affinity) than that of the CO-bound state-locked Mb (i.e., 0.2 Torr). The lowered $O_2$ affinity of the aquomet state-

(22) Szuki, T.; Imai, K. *Comp. Biochem. Physiol*. **1997**, *117B*, 599−604.
(23) Phillips, S. E. V.; Schoenborn, B. P. *Nature* **1981**, *292*, 81−82.
(24) Quillin, M. L.; Arduini, R. M.; Olson, J. S.; Phillips, G. N., Jr. *J. Mol. Biol.* **1993**, *234*, 140−155.
(25) In addition to these two structural factors, it has been suggested that the displacement of a distal pocket water molecule that is hydrogen-bonded to the $N_\epsilon$ atom of the distal His(E7−64) in deoxyMb is part of the kinetic and equilibrium barrier to ligand binding.[24] According to published data on distal heme pocket mutants of Mb, an obvious correlation exists between the presence of inhibitory distal pocket water in ferrous Mb and the observation of water coordination in the aquomet form. However, our recent findings that the optical spectral properties of the sol−gel encapsulated ferrous Mb samples can be relatively rapidly converted to those of typical, water-liganded ferric Mb upon oxidization with ferricyanide (data not shown) does not support correlation between the $O_2$ affinities of the protein conformations and the extent of water coordination in the aquomet form. Samuni et al.[18] also reported that differences in CO rebinding kinetics between two MbCO samples that were initially encapsulated in the CO-liganded and deoxy form, respectively, are retained even upon exposure to the osmotic stress of 100% glycerol. These findings argue against variation in water occupancy within the distal pocket as a source of the functional differences.
(26) Vojtechovsky, J.; Chu, K.; Berendzen, J.; Sweet, R. M.; Schlichting, I. *Biophys. J.* **1999**, *77*, 2153−2174.

locked Mb may be due to the proximal effect resulting from its high-spin iron and/or to significant differences in the distal pocket conformation between aquomet Mb and MbCO.[27] In any case, the simple monophasic $O_2$ equilibrium curve of the aquomet state-locked Mb can be well correlated with its single distal pocket conformation.

Taken together the distal heme pocket conformational population is the most probable structural explanation for the functional heterogeneity in the deoxy state-locked Mb, but more studies are necessary to provide direct evidence.

**Relation to the Physiological Function of Mb.** The data in Figure 2 show that the overall $O_2$ affinity of the deoxy state-locked Mb is significantly lower than that of the CO-bound state-locked Mb. The lowered $O_2$ affinity of the deoxy conformation is consistent with a mechanism by which deoxyMb protects against autoxidation of the heme iron. Autoxidation of Mb occurs both by direct dissociation of the neutral superoxide radical ($HO_2$) from $MbO_2$[28] and by outer-sphere electron transfer between free $O_2$ and deoxyMb containing a weakly coordinated water molecule.[29] In $MbO_2$, hydrogen bonding between bound $O_2$ and the distal His(E7−64) plays a critical role in the inhibition of autoxidation by preventing both dissociation of bound $O_2$ and its protonation.[30] On the other hand, deoxyMb inhibits autoxidation by adopting a more sterically hindered heme pocket. The increased steric hindrance can decrease the accessibility of the iron atom to solvent water molecules but may as a result hinder binding of $O_2$.

We do not know whether the above-discussed conformational multiplicity in deoxyMb is of physiological importance. However, one interesting possibility is that the relative population of the different conformations may be affected by non-heme ligands, like an allosteric protein. Evidence for Mb as an allosteric monomeric protein was presented by Giardina et al.,[31] who found that lactate, the end product of anaerobic metabolism, lowers the $O_2$ affinity by preferentially binding to Mb in the deoxy form.

## Conclusions

We have shown that the $O_2$ equilibrium properties of Mb locked in the liganded (CO-bound) and unliganded (deoxy) conformations by encapsulation in the wet sol−gel are markedly different from each other. The structural origins of the $O_2$ binding characteristics of the individual protein conformations have not yet been fully clarified, but it seems likely that the observed heterogeneity in deoxyMb is due to differences in the distal heme environment. Interestingly, the $O_2$ affinity distribution of the deoxy state-locked Mb ranges from about 0.2 to 40 Torr, comparable to that of human hemoglobin, which adopts the T and R states. These results lead us to suggest that the overall $O_2$ equilibrium properties of Mb in solution are generated by a redistribution of protein conformational populations in response to ligand binding. This conclusion is consistent with modern concepts of ligand binding and protein conformational changes,[32−34] which predict that proteins exist in an ensemble of structures, described by an energy landscape. According to this viewpoint, even a simple, monomeric protein such as Mb can assume different conformations that perform the same function but with different functional activities. Finally, our present results, together with recent findings by Friedman and colleagues,[18] suggest a general utility of the sol−gel method as a useful means for controlling the structural (functional) states of proteins, including monomeric enzymes.

**Acknowledgment.** This work was supported by a research grant (12878125) to N.S. from the Ministry of Education, Science, Sports, and Culture, Japan.

JA029237G

(27) For example, in aquomet Mb the distal His(E7−64) is present as the $N_\delta H$ tautomer, whereas in MbCO the $N_\epsilon H$ tautomer is the major isomer present.[26] The $N_\delta H$ tautomer would inhibit $O_2$ binding because of its inability to form a hydrogen bond with bound $O_2$.

(28) Shikama, K. *Biochem. J.* **1984**, *223*, 279−280.
(29) Wallace, W. J.; Houtchens, R. A.; Maxwell, J. C.; Caughey, W. S. *J. Biol. Chem.* **1982**, *257*, 4966−4977.
(30) Brantley, R. E., Jr.; Smerdon, S. J.; Wilkinson, A. J.; Singleton, E. W.; Olson, J. S. *J. Biol. Chem.* **1993**, *268*, 6995−7010.
(31) Giardina, B.; Ascenzi, P.; Clementi, M. E.; De Sanctis, G.; Rizzi, M.; Coletta, M. *J. Biol. Chem.* **1996**, *271*, 16999−17001.
(32) Frauenfelder, H.; Sligar, S. G.; Wolynes, P. G. *Science* **1991**, *254*, 1598−1603.
(33) Leeson, D. T.; Wiersma, D. A. *Nat. Struct. Biol.* **1995**, *2*, 848−851.
(34) Frauenfelder, H.; McMahon, B. H.; Austin, R. H.; Chu, K.; Gruves, J. T. *Proc. Natl. Acad. Sci. U.S.A.* **2001**, *98*, 2370−2374.